TRANSACTIONS OF THE CHINESE SOCIETY FOR AGRICULTURAL MACHINERY
Vol. 47, No. 5, 2016

doi:10.6041/j.issn.1000-1298.2016.05.001

Simulation and Test of Grape Fruit Cluster Vibration for Robotic Harvesting

Liu Jizhan[1] Tang Shanqi[1] Shan Shuai[2] Ju Jin[1] Li Mao[1] Zhu Xinxin[1]

(1. *Key Laboratory of Modern Agriculture Equipment and Technology*, *Ministry of Education*, *Jiangsu University*, *Zhenjiang* 212013, *China*
2. *School of Mechanical Engineering*, *Jiangsu University*, *Zhenjiang* 212013, *China*)

Abstract: To reduce the serious vibration and fruit dropping that may occur in high-speed robotic harvesting of fruit clusters, a simulation model of fruit cluster vibration is necessary to vibration law discovery, influencing factor analysis and optimal control study. To achieve all of the above objectives, the simulation model must take into account of the individual difference of component properties and embody the complex multilevel stem structure, multiple fruits distribution and multiplex excitation transmission. Therefore, a flexible rod-hinge-rigid rod-mass composite model was first put forward based on the structure of stem-fruit system of grape cluster, and viscoelastic property of hinges and bending property of main spike-stalk were determined by large sample tests. Then, simulation model of grape fruit cluster was constructed by reconstitution of the solid stem system with 3D laser scan, replacement of main spike-stalk with flexible rod, random addition of fruits and definition of different components according to their normal distribution from the above test results. The accuracy of the simulation model was verified by experiments, and error of the mean value and standard deviation of fruit relative swinging angle under different excitation methods are within 2% and 6.6%, respectively. Finally, the effects of various excitation methods and harvesting stages on cluster vibration were analyzed with this model. To conclude, the successful establishment of this simulation model of grape fruit cluster provides an excellent analytical tool for robotic low-vibration and anti-fall harvesting of various fruit clusters.

Key words: grape; harvesting robot; fruit cluster; vibration; simulation model

0 Introduction

Based on the practicability of gripping, 'rachis gripping and cutting' is adopted in most of the existing researches on fruit cluster robotic harvesting of grapes, litchis and etc[1-6]. However, the movement of high-speed picking and transferring during robotic harvesting may cause vibration of clusters and lead to fruits' falling[7]. Unexpected fruit falling caused by vibration is regarded as one of main obstacles to successful and efficient robotic harvesting.

To solve the above problem, study of cluster vibration properties is essential. Generally a given excitation transmitting through the 'branch-stem-fruit' system makes fruits vibrate and lead to fruit falling if force between any fruit and stem exceeds the detaching threshold. To discover the vibration mechanism, many scholars have been engaged in mechanical modeling of 'stem-fruit' system. For example, UPADHYAYA, et al[8-9], adopted a simple pendulum model to analyze the 'stem-fruit' system, while AWADY, et al[10], regarded a 'stem-fruit' system as a 'spring-mass' system in consideration of the elasticity of stem. RAND, et al[11], took account of the mass and rigidity of stalks and used a structure of stem-mass hinged to branch to describe the coupled vibration relations of 'branch-fruit-stem'. BENTAHER, et al[12], regarded the 'fruit-stem' system as a cantilever-mass structure in the finite element simulation, while COOKE, et al[13], described the bending deformation of stem and the relative elastic rotation among branch, stem and fruit by adding a spring between the rod and mass. PARCHOMCHUK, et al[14], furtherly optimized this model by adding damping at the joint.

Received date: 2015-10-14 Accepted date: 2015-11-23

Supported by National Natural Science Foundation of China (Grant No. 51475212), Priority Academic Program Development of Jiangsu Higher Education Institutions (PAPD), Natural Science Foundation of Jiangsu Province (Grant No. BK20151339) and Undergraduate Research Project of Jiangsu University (Grant No. Y13A089)

Corresponding author: Liu Jizhan, Professor. E-mail: liujizhan@163.com. Tel: +86-511-88797338.

It is obvious that the above researches either aimed at single stem-fruit modeling or regarded the cluster as a whole[15]. Furthermore, they were all applied to the vibration harvesting of fruits. Compared with single stem-fruit system, the fruit cluster system has some special features, such as structure of multi-stage stalks, distribution of multiple fruits, multiplex excitation transmission and individual differences. Additionally, all of excitation sources, characteristics, positions, transmissions and the resulted form of falling off by vibration are obviously different between the robotic harvesting and the mechanized vibration harvesting of fruits.

Therefore, this paper presented a mechanical and simulation model of grape fruit cluster according to the special excitation characteristics of robotic ‘rachis gripping and cutting’ harvesting. This study provides an excellent analytical tool for achieving the robotic ‘milder vibration and less falling’ harvesting of various fruit clusters.

1 ‘Stalk-fruit’ mechanical model of fruit cluster

1.1 ‘Stalk-fruit’ structure of the cluster

Taking ‘Red globe’ grape as example, there are about 40 ~ 80 fruits in one cluster, and each fruit weights 10 ~ 25 g. Every cluster has several sub-rachises separated from the main rachis and every sub-rachis has several stems with attached fruits. During the process of robotic harvesting, the excitation was applied at gripping position of a main rachis by the end-effector, and then transmits through sub-rachis, stems, and finally to the fruits.

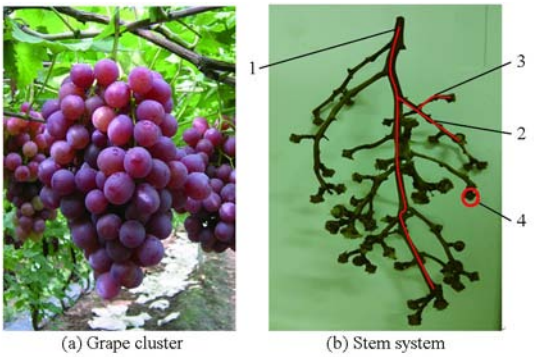

(a) Grape cluster (b) Stem system

Fig. 1 Stem-fruit structure of grape cluster

1. Main rachis 2. Sub-rachis 3. Stem 4. Pedicel

1.2 Composite mechanical model of cluster

The robotic ‘rachis gripping and cutting’ harvesting process consists of two phases. In the first picking phase, theend effector grips the main rachis and then cuts it off. And then in the second transferring phase, the manipulator transfers the end effector with gripped fruit cluster from the picking position to the unloading position.

In the two phases, excitations will transmit both by the end effector to a rachis, but characteristics of the excitations and response of the cluster are obviously different. In order to express the transmission of excitation and clusters’ responses in these two phases, a composite model of ‘flexible bar-hinge- rigid bar-spherical mass’ is proposed in this paper. In this model, the main rachis is regarded as a flexible bar to express its larger bending deformation under the vibration excitation, while the sub-rachises and stems are simplified as rigid bars. And then, the primary hinges are used to describe both deformation of sub-rachises and their rotation relatives to the main rachis, and the secondary hinges are used to represent both deformation of stems and their rotation relatives to the sub-rachises (Fig. 2a). In the picking phase, the main rachis is regarded as a flexible bar fixed to the vine. While in the transferring phase, the cluster gravity G is born by end-effector and external excitation is applied to the main rachis at the gripping position (Fig. 2b). In Fig. 2a and Fig. 2b, K represents the gripping position[16-18], $F_1(t)$ and $F_2(t)$ represent external excitation in picking and transferring phases, respectively, H represents length of main rachis from top point of cluster to fixed point to the vine, and H_K represents length of main rachis from top point of cluster to the gripping position K.

1.3 Mechanical properties of hinges between stalks

1.3.1 Principle of experiment

The mechanical properties of hinges between stalks can be expressed by relationship between loaded bending moment and relative rotation angle, because it is difficult to load and measure directly. To solve the problem of property detection, an indirect experiment can be carried out. As shown in Fig. 3a, if the primary hinge is fixed meanwhile a vertical force is applied on the secondary hinge leading to relative rotation, the relation curve of force-displacement along line of the vertical force can be obtained and be transformed to the relation curve of bending moment- relative rotation

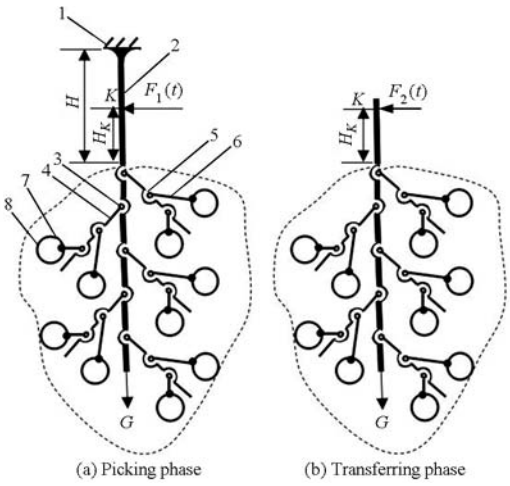

Fig. 2 Composite model of grape cluster

1. Vine 2. Flexible-bar of main rachis 3. Primary hinge 4. Sub-rachis 5. Secondary hinge 6. Stem 7. Pedicel 8. Fruit

angle.

$$M = FL \tag{1}$$

$$\theta = 90 - \theta_0 - \frac{180}{\pi}\arctan\left(\frac{\frac{L}{\tan\theta_0} - x}{L}\right) \tag{2}$$

Where, M is the bending moment loaded on the hinge, N · mm; F is the force loaded vertically on the secondary stalk, N; θ is the relative rotation angle between primary stalk and secondary stalk, (°); θ_0 is the initial angle between primary stalk and secondary stalk, (°); x is the displacement along vertical line of force F, mm; L is the horizontal distance between the line of force F and pivot of hinge, with a preset value of 35 mm.

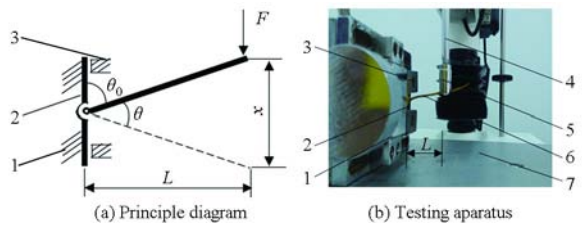

Fig. 3 Mechanical property test of hinge between stems

1. Screw-type fixture 2. Primary stalk 3. Separable clamp 4. DS – A6 adding rod 5. DS – A5 V-shape loading head 6. Secondary stalk 7. Objective table

1.3.2 Experiment materials and methods

The experiment was conducted in Key Laboratory of Modern Agricultural Equipment and Technology designated by Ministry of Education, Jiangsu University, in August, 2015 with a room temperature of 25℃. The 'Red Globe' grape clusters cultured in Ding Zhuang Village, Jurong, Zhenjiang were chosen as test samples. Seven disease-free mature grape clusters were picked at random, then 16 primary hinges and 16 secondary hinges were selected randomly after removing all fruits away. Length of all primary stalks was kept at 30 mm. All tests were carried out in 8 h after picking.

The testing apparatus included texture analyzer of TA. XTplus and screw-type fixture. As shown in Fig. 3b, the screw-type fixture was fixed on objective table of the texture analyzer vertically and both ends of the primary stalk of tested hinge sample were clamped by self-made separable clamp, then the initial angle θ_0 between the primary and secondary stalk was measured with a digital angle measuring instrument, and the diameter and length of the secondary stalk were measured with a vernier caliper. Finally the DS – A5 V-shape loading head was used to press the secondary stalk down at a constant speed of 1 mm/s vertically until the hinge was broken. The horizontal distance L between the loading position of V-shape head and pivot of the hinge was set as 35 mm, and data sampling frequency of the analyzer was set as 50 Hz.

1.3.3 Experiment results and analysis

Fig. 4a and Fig. 4b show the typical directly measured force-displacement curve and the moment-angle curve transformed by Eq. (1) and Eq. (2), respectively.

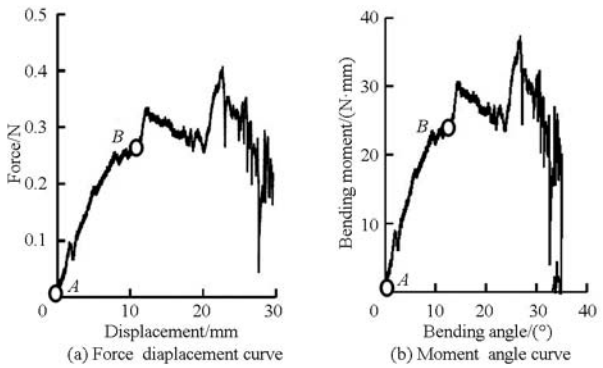

Fig. 4 Typical mechanical property curve of hinge between stems

It is found from the previous part of curve before point B that hinges between stalks present obvious viscoelastic behavior of typical agricultural materials, and then plastic deformation, yielding, reinforcement and rupture appear successively.

1.3.4 Viscoelastic model fitting

Kelvin model is a basic viscoelastic model of parallel spring-damper as follow:

$$M = E\theta + \eta \frac{\mathrm{d}\theta}{\mathrm{d}t} \tag{3}$$

Where, E is the elastic coefficient, N·mm/(°); η is the damping coefficient, N·mm·s/(°).

It can be found in Eq. (2), θ is not linear with x, which means $\mathrm{d}\theta/\mathrm{d}t$ is not a constant. In order to fitting the 'moment-angle' curve of stalks with Kelvin model, substituting Eqs. (2) into (3):

$$M = E\theta + \eta \frac{\dfrac{1}{L}}{1 + \tan^2\left(\dfrac{(\theta + \theta_0 - 90)\pi}{180}\right)} \tag{4}$$

Typical fitting result with Eq. (4) in Matlab Cftool Toolbox is shown in Fig. 5. Goodness of fit of the test data getting from all 32 samples is more than 0.93, which indicates that the model of Kelvin is ideal to express the viscoelastic characteristics of hinges among stalks.

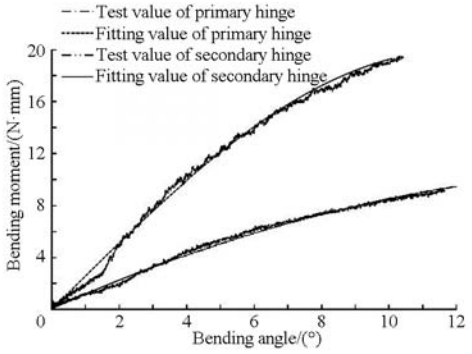

Fig. 5 Fitting results of typical moment-rotation of viscoelastic phase

1.3.5 Analysis of fitting result

From the statistical result of curve fitting of all samples, it is easy to find that the elasticity coefficients of bothprimary hinge and secondary hinge follow the normal distribution. The mean value and standard deviation of elastic coefficient of primary hinges are 3.780 and 0.729, respectively, and those of secondary hinges are 3.662 and 0.807, respectively.

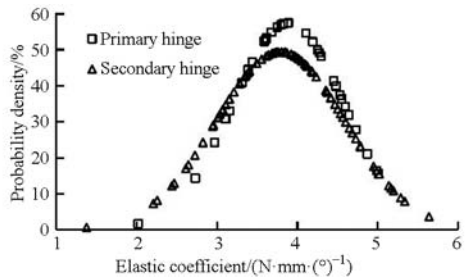

Fig. 6 Distribution of elasticity coefficient of hinges between stems

Meanwhile, obvious positive linear correlation between elasticity coefficients and damping coefficients of hinges can be found (Fig. 7).

$$\eta_1 = 0.64E_1 + 0.72 \quad (R^2 = 0.922) \tag{5}$$

$$\eta_2 = 0.62E_2 + 0.16 \quad (R^2 = 0.870) \tag{6}$$

Where, E_1 is elasticity coefficient of primary hinge, N·mm/(°); η_1 is damping coefficient of primary hinge, N·mm·s/(°); E_2 is elasticity coefficient of secondary hinge, N·mm/(°); η_2 is damping coefficient of secondary hinge, N·mm·s/(°).

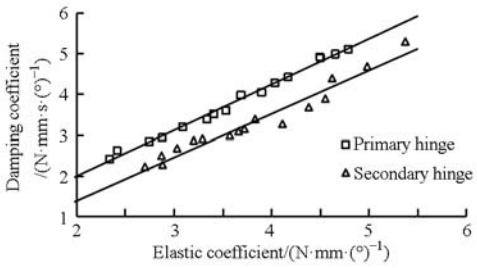

Fig. 7 Relation between elasticity and damping coefficient of hinges between stems

1.4 Flexural properties of rachis

1.4.1 Material and methods

In these tests, materials and apparatus were the same as used in section 1.3. To carry out bending tests of simply supported beam, seven rachises were randomly chosen and cut off to assure length of 160 mm (Fig. 8). Then diameters of both ends and middle part of each rachis were measured with vernier caliper and their mean values were regarded as its cross section diameter. Later each rachis was pressed down slowly at a speed of 1 mm/s on the middle part with the V-shape loading head. When the force reached 1.5 N, the loading head was stopped and kept loading for 10 s.

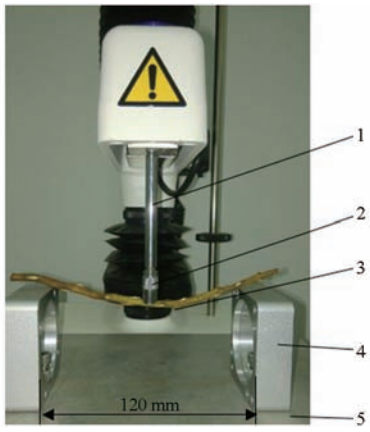

Fig. 8 Bending test of main rachis-stalk

1. DS-A6 adding rod 2. DS-AS V-shape loading head 3. Main rachis 4. Support element 5. Objective table

The bending modulus E_t of rachis can be obtained by[19]

$$E_t = \frac{F_t L_t^3}{48 I \gamma} \quad (7)$$

In which,

$$I = \frac{\pi D^4}{64} \quad (8)$$

Where, F_t is the load applied to the middle part of a rachis, which was set as 1.5 N; L_t is the distance between the two support points, with a pre-set value of 120 mm; I is the moment of inertia, mm^4; γ is the deflection of rachis, mm; D is the cross section diameter of rachis, mm.

1.4.2 Test results

With obtained test data and Eqs. (7) and (8), it can be easily figured out that range of diameter, deflection, bending modulus of sampled rachises are (3.38 ± 0.34) mm, (12.18 ± 2.08) mm, (585.85 ± 17.7) MPa, respectively.

1.5 Physical properties of fruits

Test materials were the same as used in section 1.3, 100 'Red globe' grape fruits were selected randomly, whose polar and equatorial radius were measured with a vernier caliper, also their weights were obtained with an electronic balance.

Test results (Fig. 9) show that there is less difference between polar radius and equatorial radius, which indicates that the grape fruits are nearly spherical.

$$D_e = 0.95 D_p + 0.207 \quad (9)$$

Where, D_e is equatorial radius of grape fruit, mm; D_p is polar radius of grape fruit, mm.

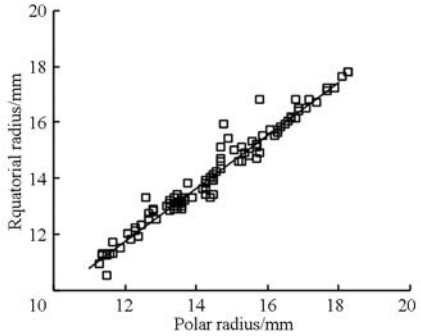

Fig. 9 Relation between equatorial and polar of fruits

Therefore, the grape fruits can be regard asballs, whose radius can be replaced by mean value of their equatorial and polar radius, respectively. Compared the volume of the grape fruits calculated as ideal balls with corresponding mass of all sampled fruits, we can find an obvious linear relation (Fig. 10).

$$m = 1.277 \times 10^{-3} V \quad (R^2 = 0.991) \quad (10)$$

Where, m is the mass of fruit, g; V is the approximate volume of fruit, mm^3.

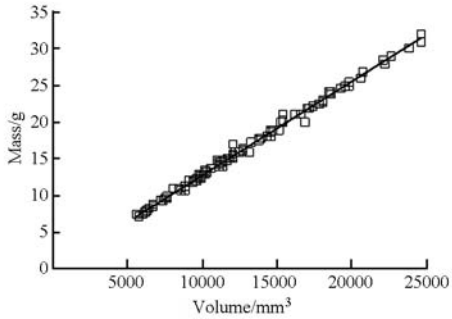

Fig. 10 Relation between mass and approximate volume of fruits

2 Simulation model of vibration

2.1 Modeling of the stalk system

Firstly, the fruits were all removed from the cluster to leave only the stalk system and put it above the induction spots, then a portable 3D scanner of Creaform EXAscan was used to get its profile (Resolution: 0.2 mm). The portable scanner was slowly moved around the stalk system until clear point-cloud images of all parts were obtained, except for the bottom part. Finally, the software of 'imagewave' was used to repair the missing parts and build the model of stalk system which could be further imported into ADMAS in x_t format. Detail scan processing and soft interface was shown in Fig. 11.

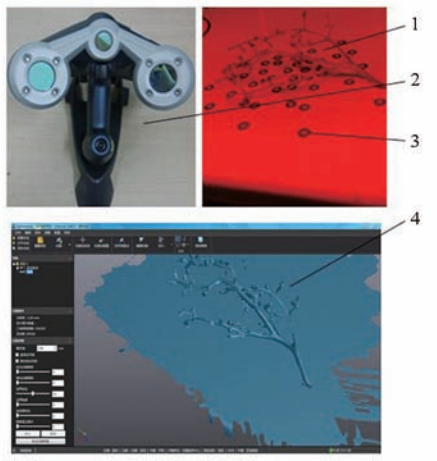

Fig. 11 3D laser scan of the stem system

1. Stem system 2. EXAscan scanner 3. Calibration point 4. Point-cloud image

2.2 Property definition of stalk system

First, parameters of the entity model of rachis

were defined in ANSYS as follows: density was 438 kg/m^3, poisson's ratio was 0.32 and elasticity modulus was 586 MPa[20-21]. Afterwards, the model was meshed, connection points were added to both ends, and the modes order was set as 18. In this way, a flexibility bar model of rachis was built and imported into ADMAS by a neutral file to replace the rachis part of stalk system model built in section 2.1. All sub-rachises and stems were regarded as rigid rods[22], whose density was also defined as 438 kg/m^3 in ADAMS to obtain a combined rigid-flexible entity model of stalk system.

2.3 Normal-addition of fruits

With NORM.INV function and RAND function in Excel, a set of normal random data of diameters was obtained according to the normal distribution law of test results in section 1.5, whose number was the same as the scanned cluster sample. Then these normally distributed diameter data would be used to build entity mass balls models of fruits, which were fixed randomly on the stems at pedicel position in the entity model of stalk system. All fruits were regarded as rigid material with density of 1 277 kg/m^3 calculated from Eq. (10).

2.4 Normal-addition of hinges between stalks

Also with NORM.INV function and RAND function in Excel, a set of normal random data of elasticity coefficient was obtained according to the normal distribution law of test results in section 1.3, whose number was the same as scanned cluster sample. Then a set of data of damping coefficient was obtained from Eqs. (5) and (6), and these normally distributed data of elasticity and damping coefficient would be used to define primary hinges and secondary hinges randomly in the entity model of stalk system.

2.5 Establishment of vibration simulation model of two phases

In view of the difference of excitations between picking phase and transferring phase, by fixing top end of the rachis and applying opposite excitation forces with same value on the rachis at gripping position, the vibration simulation model of picking phase was firstly established. And then, by adding prismatic joint at gripping position along direction of the excitation force and finishing force setting, the vibration simulation model of transferring phase was also established as shown in Fig. 12.

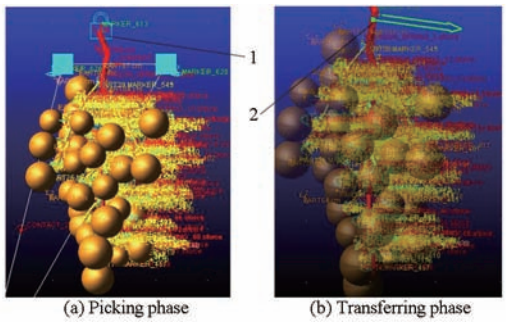

Fig. 12 Establishment of simulation cluster model

1. Frictionless fixed hinge 2. Overhanging and gripping

3 Verification of the simulation model

3.1 Running of simulation model

The new simulation model was run firstly to verify its feasibility and accuracy. With the simulation model of cluster vibration of transferring phase, H_K was set as 35 mm firstly, and an excitation of horizontal acceleration and deceleration was applied at gripping position: to accelerate at 12 m/s^2 until the speed reached 1.6 m/s and maintained the speed for 400 ms, then slowed down to 0 m/s with a deceleration of -12 m/s^2. In model running, declination angle of each fruit in vibration was selected as an important index which was defined as the angle between connecting line of gripping position and centroid of fruit and the vertical line. All fruits in the model were labeled and declination angle of each fruits was measured in vertical projective plane where the excitation laid. From statistical projective declination angles of all fruits, regulation of cluster vibration might be revealed(Fig. 13).

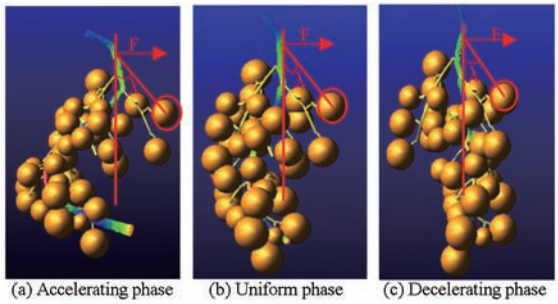

Fig. 13 Experiment of simulation cluster vibration model

3.2 Observation of vibration of cluster

The rachis of cluster was attached to a clamp to guarantee same H_K of 35 mm, which was driven by a servo motor in a horizontal linear guide. Then same excitation of horizontal acceleration and deceleration was applied on the cluster. MS3100/CIR high-speed camera was used to catch the real declination angle of

fruits (Fig. 14). The shutter speed was set as 300 frame per second. Finally pictures taking with the high-speed camera were imported to Matlab to get the value of projective declination angles by using function of 'ginput'.

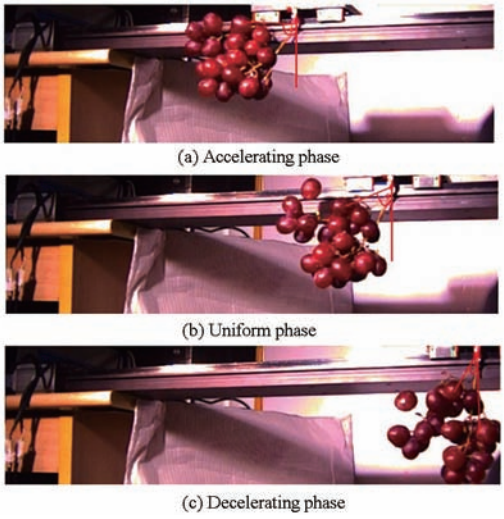

Fig. 14 Observation of cluster vibration with high-speed photography

3.3 Verification of simulation accuracy

To show the state of vibration, relative swing angle that referred to difference between the declination angle of fruits in vibration and the initial position was brought in. Statistical analysis of relative swing angles at vibration time of 100 ms in accelerating sub-phase, 300 ms in uniform motion phase and 600 ms in decelerating phase were carried out in both simulation and experiment. By comparing, it is easy to find that relative swing angles of all fruits in the cluster obey normal distribution and the distribution parameters of simulation are highly consistent with those of the experiment (Tab. 1). The differences of average value and standard deviation between simulation and experiment are within 2% and 6.6%, respectively, which indicates that the model has satisfied accuracy and can meet the demand of further research of cluster vibration well.

Tab. 1 Normal distribution of fruit swing angle

(°)

Time/ms	Simulation		Test	
	Mean value	Standard deviation	Mean value	Standard deviation
100	16.27	2.25	15.93	2.10
300	11.43	4.08	11.51	4.19
600	8.62	1.84	8.70	2.06

4 Simulation of grape cluster vibration

4.1 Difference between phases of picking and transferring

In simulation, H and H_K were set as 80 mm and 35 mm, respectively. Adding an excitation of 12 m/s^2 acceleration in horizontal direction in both picking phase and transferring phase, and the relative swing angles of all fruits at same excitation distance of 100 mm were recorded. By statistical analysis of these swing angles, it was found that angles of both picking phase and transferring phase followed the normal distribution (Fig. 15).

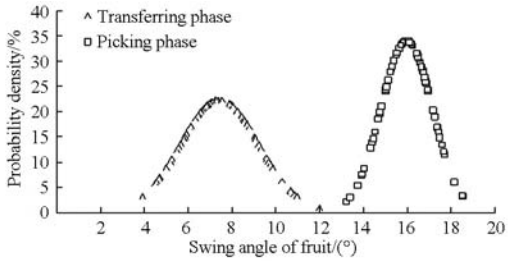

Fig. 15 Fruit swing angle at different stages

As shown in Fig. 15, the vibration amplitude in the picking phase is much greater than that in the transferring phase. It may be attributed to the lever amplification effect resulted from the fixing of top end of the rachis.

4.2 Influence of excitation characteristics on cluster vibration

4.2.1 Simulation of different excitation characteristics

With the simulation model of cluster vibration of transferring phase, three different single-factor simulation experiments were carried out when H and H_K was still set as 80 and 35 mm:

(1) Simulation running under excitation of 12 m/s^2 acceleration in both horizontal and vertical directions was carried out, and the relative swing angles at excitation distance of 400 mm were recorded.

(2) Simulation running under excitations of 6, 8, 10, 12 m/s^2 acceleration in horizontal direction was carried out, respectively, and the relative swing angles at excitation distance of 400 mm were recorded.

(3) Simulation running under excitations of 12 m/s^2 acceleration in horizontal direction was carried out, and the relative swing angles at excitation distances of 200, 300, 400 mm were recorded,

respectively.

4.2.2 Analysis of effecting factors to cluster vibration

(1) The statistical result of the relative swing angle of fruits in different directions is showed in Fig. 16. The cumulative relative swing angle reaches 722.0° for horizontal excitation, which is larger than 632.1° for vertical excitation.

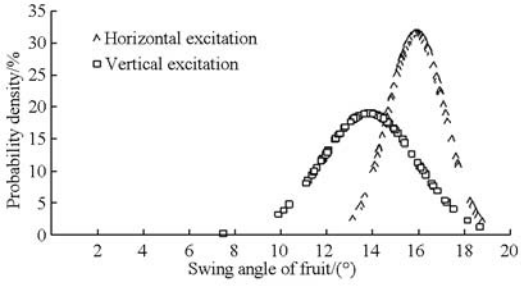

Fig. 16 Fruit swing angle under different excitation directions

(2) The statistical result of the relative swing angle of fruits in horizontal direction under different incentive intensities is showed in Fig. 17. It is found that the cumulative relative swing angles under excitation intensities of 6, 8, 10, 12 m/s^2 are 236.5°, 327.8°, 559.0° and 722.0°, respectively. It is easy concluded that the larger incentive intensity is, the greater serious vibration is.

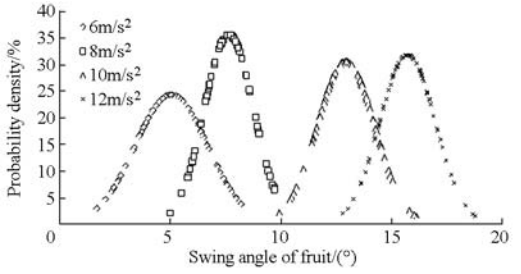

Fig. 17 Fruit swing angle under different excitation values

(3) The statistical result of the relative swing angle of fruits in horizontal direction under different excitation ranges is showed in Fig. 18. The cumulative relative swing angles are 342.5°, 468.9°, 595.7°, 722.0°, when the excitation range reached 100, 200, 300, 400 mm, respectively. Therefore, the degree of vibration is proportional to the excitation range.

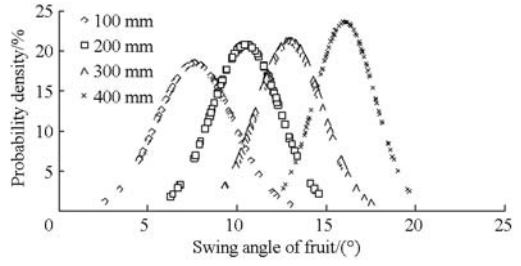

Fig. 18 Fruit swing angle under different excitation ranges

5 Conclusions

(1) In this study, the composite model of 'flexible bar-viscoelastic hinge-rigid bar-spherical mass' was proposed according to the special excitation characteristics of the robotic 'rachis gripping and cutting' harvesting, and the characteristics of all components in this model were detected by experiments.

(2) The 3D model of grape fruit cluster for vibration simulation was built by modeling of stalk system with laser scanning, replacing main rachis with flexibility bar and normal adding of fruits and hinges. The relative swing angles of simulation in both picking phase and transferring phase were recorded and differences of average value and standard deviation between simulation and experiment were found within 2% and 6.6%, respectively.

(3) By simulation of cluster vibration, it was found that the vibration in the picking phase is much greater than that in the transferring phase. With respect to the transferring phase, all factors of excitation direction, intensity and range have significant impacts on cluster vibration. According to simulation results it is believed that vibration caused by horizontal excitation is serious than vertical excitation, and the degree of vibration is proportional to both excitation intensity and range.

(4) This high-accuracy simulation model of cluster vibration will contribute greatly to the research of robotic anti-fall harvesting, and also provide an excellent analytical tool for the mechanized vibration-harvesting research field. However, limited by available method, impact among fruits has not yet been involved in.

References

[1] LIU Jizhan, LIU Wei, MAO Hanping, et al. Design and coordinated motion simulation of transplanting robot for column cultivation [J]. Transactions of the Chinese Society for Agricultural Machinery, 2014, 45(7): 48 – 53. (in Chinese)

[2] SHIGEHIKO H, KENTA S, SATOSHI Y, et al. Evaluation of a strawberry-harvesting robot in a field test [J]. Biosystems Engineering, 2010, 105(2): 160 – 171.

[3] ZHANG Kailiang, YANG Li, ZHANG Tiezhong. Design and testing of picking and execution mechanism of

strawberry harvesting robot [J]. Transactions of the Chinese Society for Agricultural Machinery, 2011, 42(9): 155 - 161. (in Chinese)

[4] BULANON D M, KATAOKA T. A fruit detection system and an end effector for robotic harvesting of Fuji apples [J]. Agricultural Engineering International: CIGR Journal, 2010, 12(1): 203 - 210.

[5] LIU Jizhan, XU Xiuqiong, LI Pingping. Analysis and experiment on laser cutting of fruit peduncles [J]. Transactions of the Chinese Society for Agricultural Machinery, 2014, 45(1): 59 - 64. (in Chinese)

[6] LIU Jizhan, BAI Xinxin, LI Pingping, et al. Complex collision model in high-speed gripping of fruit [J]. Transactions of the Chinese Society for Agricultural Machinery, 2014, 45(4): 49 - 54. (in Chinese)

[7] NAOSHI K, KOICHI T, TOMOWO S, et al. Path planning of tomato cluster harvesting robot for realizing low vibration and speedy transportation [J]. Engineering in Agriculture, Environment and Food, 2009, 2(3): 108 - 115.

[8] UPADHYYAYA S K, RAND R H J, COOKE R. Dynamics of fruit tree trunk impact [J]. Transactions of the ASAE, 1981, 24(4): 846 - 855.

[9] MOHAMED I G. Prediction of the suitable amplitude of shaking unit for fruit harvesting [J]. Misr Journal of Agriculture Engineering, 2006, 23(1): 1 - 18.

[10] AWADY M N EL, GENAIDY MA L, RASHOWAN M. Modeling and simulating of olive-tree harvesting mechanism [J]. Misr Journal of Agriculture Engineering, 2008, 25(3): 712 - 722.

[11] RAND R H, COOKE J R. Vibratory fruit harvesting: a linear theory of fruit-stem dynamics [J]. Journal of Agriculture Engineering Research, 1970, 15(4): 347 - 363.

[12] BENTAHER H, HADDAR M, FAKHFAKH T. Finite elements modeling of olive tree mechanical harvesting using different shakers [J]. Trees, 2013, 27(6): 1537 - 1545.

[13] COOKE J R, RAND R H. Vibratory fruit harvesting: a linear theory of fruit-stem dynamics [J]. Journal of Agriculture Engineering Research, 1969, 14(3): 195 - 209.

[14] PARCHOMCHUK P, COOKE J R. Vibratory harvesting: an experimental analysis of fruit - stem dynamics [J]. Transactions of the ASAE, 1971, 14(1): 20 - 24.

[15] LI Yongqiang, YANG Xuejun, WANG Jun, et al. Simulation of wine grape plants forced vibration based on ADAMS [J]. Journal of Anhui Agricultural Sciences, 2015, 43(27): 220 - 224. (in Chinese)

[16] LUO Lufeng, ZOU Xiangjun, XIONG Juntao, et al. Automatic positioning for picking point of grape picking robot in natural environment [J]. Transactions of the CSAE, 2015, 31(2): 14 - 21. (in Chinese)

[17] LU Jun. The association positioning of picking-machine and vision based on virtual design [D]. Guangzhou: South China Agricultural University, 2009: 60 - 64. (in Chinese)

[18] XIONG Juntao, ZOU Xiangjun, CHEN Lijuan, et al. Recognition of mature litchi in natural environment based on machine vision [J]. Transactions of the Chinese Society for Agricultural Machinery, 2011, 42(9): 162 - 166. (in Chinese)

[19] WANG Rong. Research on the dynamical properties and mechanical damage of grape and tomato [D]. Beijing: China Agricultural University, 2003. (in Chinese)

[20] WANG Rong, JIAO Qunying, WEI Deqiang. Determination of the macroscopic mechanical properties of grape and tomato [J]. Transactions of the CSAE, 2004, 20(2): 54 - 57. (in Chinese)

doi:10.6041/j.issn.1000-1298.2016.05.001

机器人采摘葡萄果穗振动仿真与试验

刘继展[1]　唐善奇[1]　单　帅[2]　居　锦[1]　李　茂[1]　朱新新[1]

(1. 江苏大学现代农业装备与技术教育部重点实验室, 镇江 212013; 2. 江苏大学机械工程学院, 镇江 212013)

摘要: 针对机器人摘取及移送过程中导致的果穗振动与果粒脱落问题,提出了一种面向穗轴激励输入的果穗振动仿真模型。以葡萄为研究对象,在果穗"梗-果"结构特性基础上,提出了"挠性杆-铰链-刚性杆-质量球"复合果穗模型,并由试验确定了模型中各级梗间铰链弹性系数与阻尼系数、果粒尺寸与质量的正态分布规律,获得了主穗轴的抗弯特性。进而利用激光 3D 扫描重构得到梗系统,根据试验结果分别进行刚性、挠性杆件定义和果粒与梗间铰链的添加,构建得到果穗振动仿真模型。通过仿真精度验证试验发现,在激励作用的加速、匀速和减速阶段,经正态分布统计仿真与实测中果穗的各果粒摆角均值与标准差相差均在 2% 和 6.6% 以内,表明不同阶段其精度均良好。最终利用该模型分析了不同激励方式及不同采摘阶段对果穗振动的影响。果穗振动仿真模型的建立,为实现各类果穗的机器人"减振低脱"采摘提供了有力的分析工具。

关键词: 葡萄; 采摘机器人; 果穗; 振动; 仿真模型

中图分类号: TP242　　**文献标识码**: A　　**文章编号**: 1000-1298(2016)05-0001-08

Simulation and Test of Grape Fruit Cluster Vibration for Robotic Harvesting

Liu Jizhan[1]　Tang Shanqi[1]　Shan Shuai[2]　Ju Jin[1]　Li Mao[1]　Zhu Xinxin[1]

(1. *Key Laboratory of Modern Agriculture Equipment and Technology*, *Ministry of Education*, *Jiangsu University*, *Zhenjiang* 212013, *China*

2. *School of Mechanical Engineering*, *Jiangsu University*, *Zhenjiang* 212013, *China*)

Abstract: To reduce the serious vibration and fruit dropping that may occur in high-speed robotic harvesting of fruit clusters, a simulation model of fruit cluster vibration is necessary to vibration law discovery, influencing factor analysis and optimal control study. To achieve all of the above objectives, the simulation model must take into account of the individual difference of component properties and embody the complex multilevel stem structure, multiple fruits distribution and multiplex excitation transmission. Therefore, a flexible rod-hinge-rigid rod-mass composite model was first put forward based on the structure of stem-fruit system of grape cluster, and viscoelastic property of hinges and bending property of main spike-stalk were determined by large sample tests. Then, simulation model of grape fruit cluster was constructed by reconstitution of the solid stem system with 3D laser scan, replacement of main spike-stalk with flexible rod, random addition of fruits and definition of different components according to their normal distribution from the above test results. The accuracy of the simulation model was verified by experiments, and error of the mean value and standard deviation of fruit relative swinging angle under different excitation methods are within 2% and 6.6%, respectively. Finally, the effects of various excitation methods and harvesting stages on cluster vibration were analyzed with this model. To conclude, the successful establishment of this simulation model of grape fruit cluster provides an excellent analytical tool for robotic low-vibration and anti-fall harvesting of various fruit clusters.

Key words: grape; harvesting robot; fruit cluster; vibration; simulation model

收稿日期: 2015-10-14　修回日期: 2015-11-23

基金项目: 国家自然科学基金项目(51475212)、江苏高校优势学科建设工程项目(PAPD)、江苏省自然科学基金项目(BK20151339)和江苏大学第 13 批大学生科研立项(Y13A089)

作者简介: 刘继展(1976—),男,研究员,博士,主要从事农业机器人研究,E-mail: liujizhan@163.com

引言

基于夹持的可实施性,现有葡萄、荔枝等成串果实的机器人收获[1]大多采用“穗轴夹剪”方式[1-6]。但是在机器人采摘作业时,快速摘取与移送动作均可能引起悬挂果穗的振荡进而导致果粒的脱落[7],果粒的振动脱落成为严重影响机器人采摘成功率与效率的主要因素。其中,对果穗的振动特性研究是解决快速采摘中果粒防脱落问题的基础和关键。

特定激励经过枝干-梗-果系统的传递引起果实的振动,当梗-果连接部位应力超过其强度时即导致果粒的脱落。在梗-果系统模型方面,UPADHYYAYA 等[8-9]应用单摆模型来进行梗-果系统的分析,AWADY 等[10]则考虑果梗的弹性,将梗-果系统作为弹簧-质量块系统来分析;RAND 等[11]计入果梗自身的质量与刚度,用铰接于枝干的杆-质量块结构来描述枝-果-梗间的耦合振动关系;BENTAHER 等[12]在有限元仿真中将果-梗系统处理为悬臂梁-质量块结构;COOKE 等[13]则将杆-质量块系统的连接点进一步附加弹簧,从而描述了果梗的弯曲变形以及枝-梗-果间的弹性相对转动;而后 PARCHOMCHUK 等[14]又进一步对该模型进行了优化,在关节处添加了阻尼。

但是,现有研究均为单果力学模型,或将果穗简化为整体[15],且均以振动落果式收获为目标。而果穗系统存在复杂的多级梗结构、多果粒分布和激励的多路多级传递,果穗各单元间亦存在物理和力学特性的个体差异性。同时,机器人采摘过程中的激励源及激励特性、激励部位与传递路线以及果实振动脱落形式均与振动落果式收获存在着巨大的差异。为此,本文针对机器人“穗轴夹剪”采摘中的特殊激励特性,以葡萄为对象建立果穗的力学与仿真模型,从而为实现各类果穗的机器人“减振低脱”采摘提供有力的分析工具。

1 果穗“梗-果”系统力学模型

1.1 果穗“梗-果”系统结构

如图 1 所示,以红地球品种为例,每一葡萄果穗有 40 ~ 80 个果粒,果粒质量在 10 ~ 25 g 之间。每一果穗由主穗轴分出若干分枝穗轴,每一分枝穗轴进一步分出的若干果柄经果蒂与果粒连接。在机器人采摘过程中,激励通过末端执行器夹持部位经过主穗轴、分枝穗轴、果柄传递至果粒。

1.2 果穗复合力学模型

果穗的机器人穗轴夹剪采摘包括摘取与移送 2 个阶段,即先由末端夹持并剪断主穗轴,进而机械臂运动将末端与果穗从采摘位置移送至放果位置。2 个阶段的振动激励均经过末端传递给主穗轴,但 2 个阶段的激励与果穗响应特性存在明显差异。为充分表征 2 个阶段的激励传递与果穗响应,提出了“挠性杆-铰链-刚性杆-质量球”复合果穗模型。其中,以挠性杆表征主穗梗在振动激励下的较大弯曲变形;而将分枝穗梗、果柄视为刚性杆,进而以 1 级铰链表征振动激励下分枝穗梗的弯曲变形及其与主穗梗间的相对转动,以 2 级铰链表征分枝穗梗与果柄的弯曲变形以及二者间的相对转动。摘取阶段主穗轴和枝干的连接方式为挠性杆和机架固定连接(图 2a),而移送阶段主穗轴则在夹持部位由末端承受果穗重力 G 并受到外部激励(图 2b)。其中 K 为摘取点夹持部位[16-18],$F_1(t)$、$F_2(t)$分别为摘取、移送阶段的外部激励,H 为外伸穗轴长,H_K为夹持穗轴长。

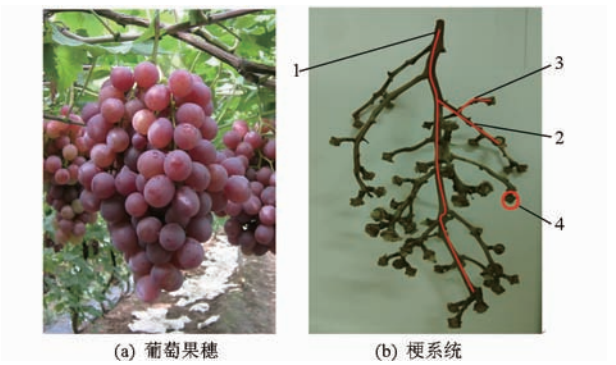

图 1 葡萄果穗“梗-果”系统结构示意图

Fig. 1 Stem-fruit structure of grape cluster

1. 主穗轴 2. 分枝穗轴 3. 果柄 4. 果蒂

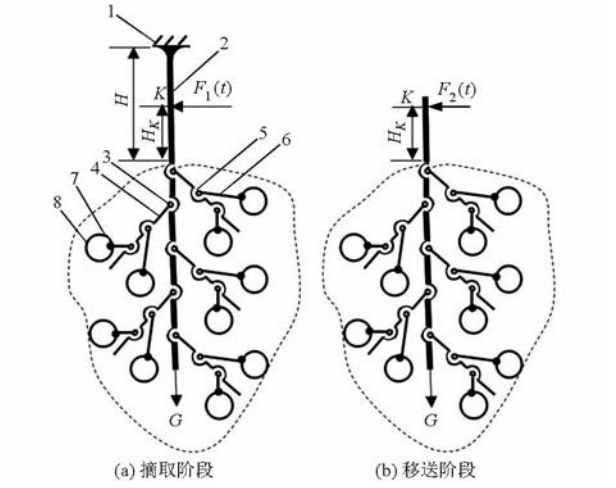

图 2 “挠性杆-铰链-刚性杆-质量球”复合果穗模型

Fig. 2 Composite model of grape cluster

1. 枝干 2. 主穗轴挠性杆 3. 1 级铰链 4. 分枝穗轴 5. 2 级铰链 6. 果柄 7. 果蒂 8. 果粒

1.3 梗间铰链力学特性

1.3.1 试验原理

梗间铰链的力学特性表现为弯矩-转角关系,但弯矩-转角的直接加载和测定困难,因而进行了间接

加载试验。如图 3a 所示，固定梗间铰链的上级梗，并对下级梗进行竖直加载，从而获得力-位移曲线，并进而将其转换为弯矩-转角曲线。

$$M = FL \tag{1}$$

$$\theta = 90 - \theta_0 - \frac{180}{\pi}\arctan\left(\frac{\frac{L}{\tan\theta_0} - x}{L}\right) \tag{2}$$

式中　M——梗间铰链加载弯矩，N·mm

F——施加于下级梗的竖直作用力，N

L——力 F 竖直作用线与铰链中心点的水平距离，取 35 mm

θ——受载后梗间铰链上、下级梗间转角，(°)

θ_0——梗间铰链上、下级梗间初始夹角，(°)

x——下级梗沿竖直作用力 F 方向位移，(°)

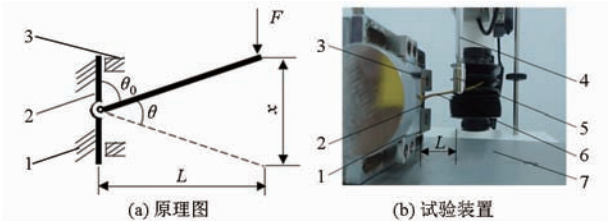

图 3　梗间铰链力学特性测定试验

Fig. 3　Mechanical property test of hinge between stems

1. 螺旋式夹具　2. 上级梗　3. 分离式夹块　4. DS－A6 型加长杆　5. DS－A5 型内凹 V 形测头　6. 下级梗　7. 载物台

1.3.2　试验材料与方法

试验于 2015 年 8 月在江苏大学现代农业装备与技术教育部重点实验室进行，室温 25℃。试验品种选择镇江市句容丁庄葡萄园培育的红地球，随机采取 7 串无虫害的全熟期葡萄果穗，摘除果粒后随机截取 1 级铰链与 2 级铰链各 16 个，使各铰链中上一级梗的两端长度均为 30 mm。全部试验于采摘后 8 h 内完成。

试验装置由 TA. XTplus 型质地分析仪和螺旋式夹具构成。如图 3b 所示，螺旋式夹具竖直固定于质地分析仪的载物台上，由自制分离式夹块夹紧铰链上级梗的两端，并利用数显角度测量仪测定上、下级梗间的初始夹角 θ_0，利用游标卡尺测量下级梗的直径与长度。应用 DS－A5 型内凹 V 形测头，以 1 mm/s 速度对该铰链的下一级梗进行竖直下压至铰链完全断裂。V 形测头竖直下压位置与铰链中心点的水平距离 L 为 35 mm，数据采样频率是 50 Hz。

1.3.3　试验结果与分析

图 4 为测得的梗间铰链典型力-位移曲线和利用式(1)、(2)折算得到的弯矩-弯角曲线。

由图 4 发现，梗间铰链在 B 点之前体现出农业物料的典型粘弹特征，B 点之后则陆续出现塑形、屈服、塑性强化直至断裂。

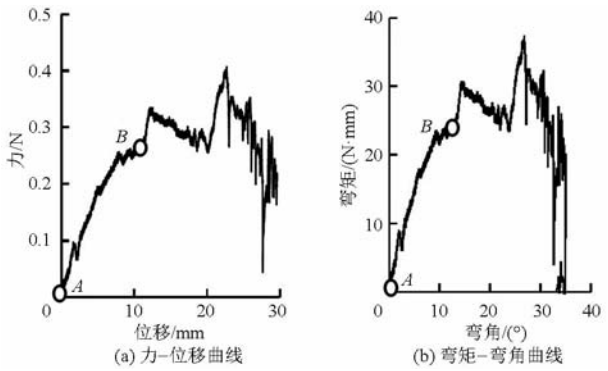

图 4　梗间铰链典型力学特性曲线

Fig. 4　Typical mechanical property curve of hinge between stems

1.3.4　粘弹模型拟合

Kelvin 模型为基本的弹簧-阻尼并联粘弹模型。

$$M = E\theta + \eta\frac{\mathrm{d}\theta}{\mathrm{d}t} \tag{3}$$

式中　E——弹性系数，N·mm/(°)

η——阻尼系数，N·mm·s/(°)

t——试验时间

由式(2)发现，试验中转角 θ 与位移 x 并非线性关系，为用试验获得的梗间铰链弯矩-转角曲线进行 Kelvin 模型拟合，结合式(2)、(3)可得

$$M = E\theta + \eta\frac{\frac{1}{L}}{1 + \tan^2\left(\frac{(\theta + \theta_0 - 90)\pi}{180}\right)} \tag{4}$$

利用 Matlab cftool 工具箱，以式(4)对试验结果进行拟合，典型拟合结果如图 5 所示。1 级铰链与 2 级铰链各 16 个样本试验结果的拟合优度均大于 0.93，表明 Kelvin 模型能够良好表征各关节的粘弹特征。

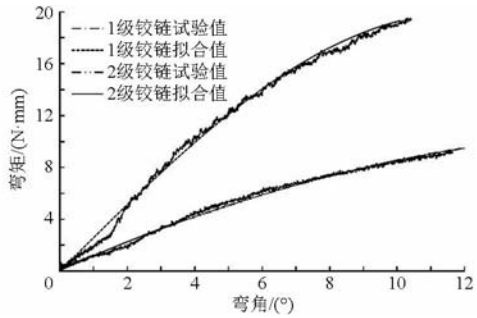

图 5　典型粘弹阶段弯矩-弯角拟合结果

Fig. 5　Fitting results of typical moment－rotation of viscoelastic phase

1.3.5　拟合结果分析

统计拟合结果发现，1、2 级铰链的弹性系数均满足正态分布(图 6)，其中 1 级铰链弹性系数的均值与标准差分别为 3.78 和 0.729，2 级铰链弹性系

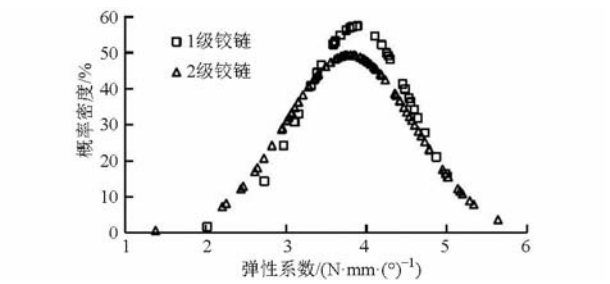

图 6 梗间铰链弹性系数统计

Fig. 6 Distribution of elasticity coefficient of hinges between stems

数的均值与标准差分别为 3.622 和 0.807。

同时发现(图 7),各级铰链间的弹性系数与阻尼系数间存在明显的线性正相关。

$$\eta_1 = 0.64E_1 + 0.72 \quad (R^2 = 0.922) \tag{5}$$

$$\eta_2 = 0.62E_2 + 0.16 \quad (R^2 = 0.870) \tag{6}$$

式中 E_1——1 级铰链弹性系数,N·mm/(°)

η_1——1 级铰链阻尼系数,N·mm·s/(°)

E_2——2 级铰链弹性系数,N·mm/(°)

η_2——2 级铰链阻尼系数,N·mm·s/(°)

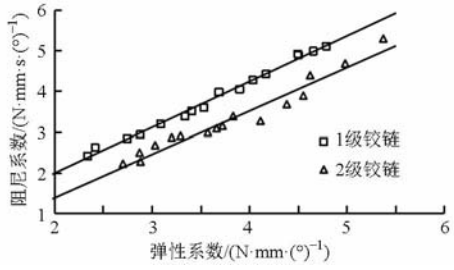

图 7 梗间铰链弹性系数-阻尼系数关系

Fig. 7 Relation between elasticity and damping coefficient of hinges between stems

1.4 主穗轴抗弯特性

1.4.1 试验材料与方法

试验材料与仪器同 1.3 节,随机选取 7 串主果穗并从每串主果穗中截取长为 160 mm 的主穗轴截段,进行简支梁的弯曲试验(图 8)。用游标卡尺分别测量主穗轴两端与中部直径,并取其平均直径为截面直径,进而用凹形压头在穗轴中心竖直加载,以 1 mm/s 初始速度缓慢加载,直至载荷达到 1.5 N 并保持 10 s。

主穗轴的弯曲模量 E_t 为[19]

$$E_t = \frac{F_t L_t^3}{48 I \gamma} \tag{7}$$

其中

$$I = \frac{\pi D^4}{64} \tag{8}$$

式中 F_t——主穗轴中部集中载荷,设定为 1.5 N

L_t——支承件间距,设定为 120 mm

I——惯性矩,mm^4 γ——主穗轴挠度,mm

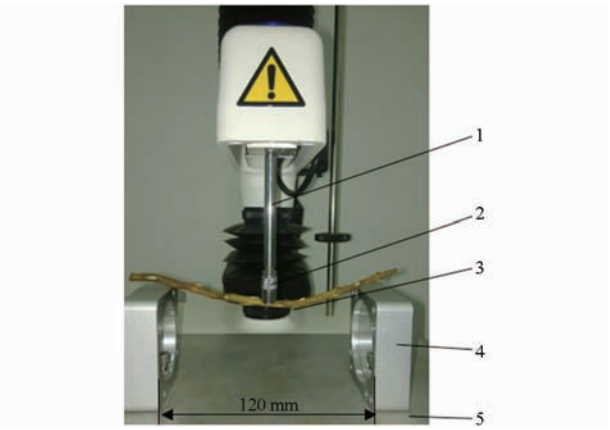

图 8 主穗轴挠性弯曲试验

Fig. 8 Bending test of main spike-stalk

1. DS-A6 型加长杆 2. DS-A5 型内凹 V 形测头 3. 主穗轴 4. 支承件 5. 载物台

D——主穗轴截面直径,mm

1.4.2 试验结果

利用压头力-位移曲线及式(7)、(8)计算发现,主穗轴各样本截面直径、挠度和弯曲模量的范围分别为(3.38 ± 0.34) mm、(12.18 ± 2.08) mm 和(585.85 ± 17.7) MPa。

1.5 果粒物理特性

试验材料同 1.3 节,随机选取 100 个果粒试样,分别用游标卡尺对其极半径、赤道半径进行测量,并用电子天平称量果粒质量。

由图 9 所示测量结果发现,红地球的果粒极半径与赤道半径差异很小,接近球形。

$$D_e = 0.95D_p + 0.207 \tag{9}$$

式中 D_e——赤道半径,mm

D_p——极半径,mm

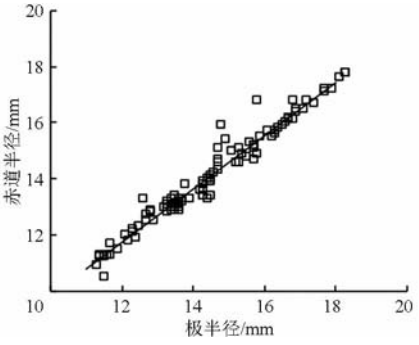

图 9 果粒赤道半径-极半径关系

Fig. 9 Relation between equatorial and polar of fruits

将果粒近似为球形,并以果粒极半径、赤道半径均值为半径求得其近似体积,则果粒近似体积与质量间呈高度线性相关(图 10)。

$$m = 1.277 \times 10^{-3} V \quad (R^2 = 0.991) \tag{10}$$

式中 m——单个果粒质量,g

V——单个果粒的近似体积,mm^3

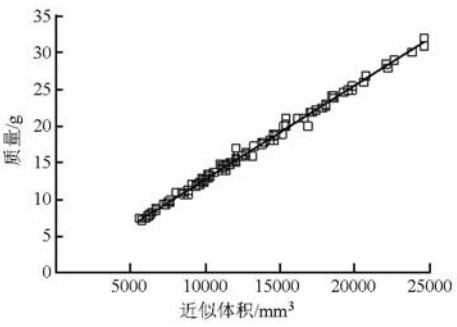

图 10　果粒质量-近似体积关系

Fig. 10　Relation between quality and approximate volume of fruits

2　果穗振动仿真模型建立

2.1　梗系统实体建模

利用 Creaform EXAscan 型激光三维扫描仪扫描葡萄果穗去除果粒后的梗系统，试验材料同 1.3 节。扫描仪设置：分辨率、解析度均为 0.2 mm，边界优化为 50。扫描时，保证梗系统平放在感应点上方同时位置固定不变，且过程中至少有 3 个感应点能被检测到。手持扫描仪从梗系统上方与四周不同角度缓慢扫描，直至除正对感应点的底面缺失外其余外表面均完全被扫描且点云图轮廓清晰，进而用软件 imagewave 进行梗系统底部缺损面的修复并建立实体，实体以 x_t 格式导入 ADAMS。扫描仪器方式及软件处理界面如图 11 所示。

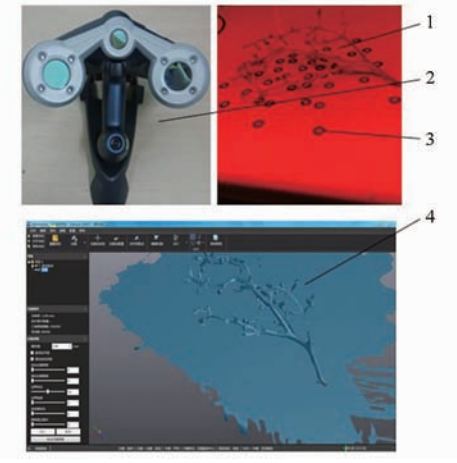

图 11　梗系统的 3D 激光扫描

Fig. 11　3D laser scan of stem system

1. 梗系统　2. EXAscan 型扫描仪　3. 感应点　4. 获取的点云图

2.2　梗系统属性定义

根据主穗轴抗弯特性试验结果，在 ANSYS 中先设定其物理参数，其中密度测得为 438 kg/m^3，泊松比取 0.32[20-21]，弹性模量则取弯曲模量测量均值 586 MPa。再进行网格划分及在主穗轴首尾端面添加外部连接点，同时设置其模态数（本文模型为 18 阶）与单位，建立主穗轴的挠性杆模型，并通过生成中性文件将其导入 ADAMS，替换 2.1 节所建立梗系统实体模型中的主穗轴。进而进行分枝穗轴与果柄的材料参数定义：密度为 438 kg/m^3，弹性模量与泊松比按刚性材料添加[22]，从而得到刚柔复合的梗系统实体模型。

2.3　果粒的正态添加

根据 1.5 节果粒物理特性试验获得的果粒平均直径与质量正态分布规律，利用 Excel 的 NORM.INV 与 RAND 函数组合产生与模型果粒个数一致的果粒直径正态随机数，从而在 2.2 节所建立梗系统模型的果蒂位置进行 3D 空间的果粒球体模型随机添加。同时使果粒质心、果柄质心以及果蒂 3 点共线，果粒与果柄在果蒂位置用固定副连接。根据式(10)将果粒密度设置为 1 277 kg/m^3，弹性模量与泊松比按刚性材料添加。

2.4　梗间铰链的正态添加

根据 1.3 节获得的梗间铰链特性正态分布规律，利用 Excel 的 NORM.INV 与 RAND 函数组合产生与模型中 1 级、2 级铰链个数一致的弹性系数正态随机数，进而根据式(5)、(6)获得相应铰链的阻尼系数，在各相邻梗所在平面内，依据其级别进行各级铰链弹性系数和对应阻尼系数的随机添加。

2.5　分阶段振动仿真模型

针对摘取和移送阶段主穗轴所受激励形式的不同，将主穗轴上端固定于一点，方向垂直于栅格面，两端夹块激励设置大小一致、方向相反，建立摘取阶段的果穗振动仿真模型；将夹块夹持位置设为激励作用点，在激励点先设置沿激励方向的移动副，再添加驱动设置所需激励大小，建立移送阶段的果穗振动仿真模型，如图 12 所示。

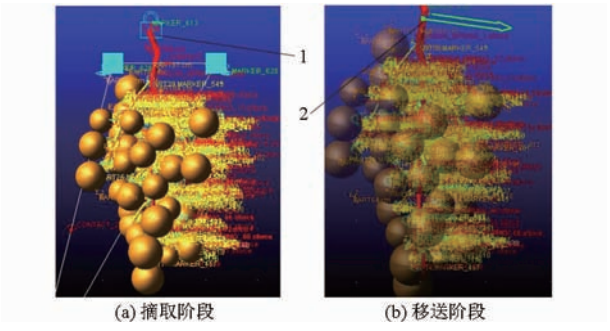

图 12　果穗振动仿真模型

Fig. 12　Establishment of simulation cluster model

1. 无摩擦铰接固定铰链　2. 悬垂夹持

3　模型合理性验证

3.1　仿真模型运行

利用建立的移送阶段果穗振动仿真模型进行直线加减速激励振动试验。设定夹持穗轴长 H_K 为

35 mm,加载方向为水平方向,激励加载方式为:首先以 12 m/s^2 使激励部位加速到 1.6 m/s 并保持 400 ms,再以 -12 m/s^2 使其减速到零。对每个果粒进行标记,设激励作用点、果粒质心所构直线与铅垂线夹角为果粒偏角,并在水平激励所处竖直平面内完成各果粒偏角投影的测量,以此表征激励作用下的果穗摆动情况(图 13)。

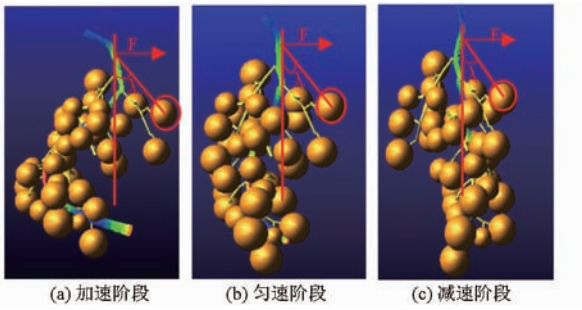

图 13 果穗振动仿真试验

Fig. 13 Experiment of simulation cluster vibration model

3.2 振动观测试验

将直线模组水平固定,由固定于滑台上的钳口夹具夹持主穗轴,并通过 PLC 设置与仿真运行一致的激励加载方式。其中夹持穗轴长 H_K 同样为 35 mm。使 MS3100/CIR 型高速摄像机垂直于直线模组水平运动所处竖直平面进行运动过程的拍摄,拍摄速度为 300 帧/s(图 14)。图片导入 Matlab 后,使用 ginput 语句抓取特征点求取各果粒偏角的投影值。

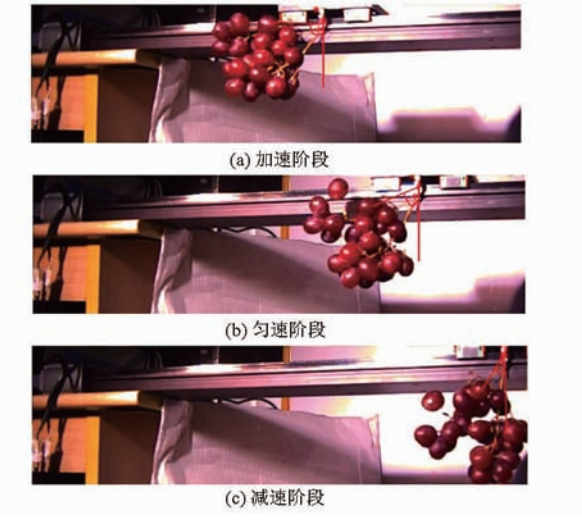

图 14 果穗振动的高速摄影观测

Fig. 14 Observation of cluster vibration with high-speed photography

3.3 仿真精度验证

令果粒在振动过程与其初始位置的相对偏角为果粒摆角,分别取仿真与试验中加速、匀速与减速阶段中的 100 ms、300 ms、600 ms 相同时刻,对竖直面内不同时刻的所有可观测果粒的摆动情况进行统计。各时刻的实测与仿真模拟结果表明(表 1),果穗中果粒摆角满足正态分布,且仿真与实测的对应正态分布参数高度吻合,其果粒摆角均值与标准差相差分别在 2% 和 6.6% 以内,表明该果穗振动仿真模型精度可满足研究的需要。

表 1 果粒摆角正态分布规律统计

Tab. 1 Normal distribution of fruit swing angle

(°)

时刻/	仿真		实测	
ms	均值	标准差	均值	标准差
100	16.27	2.25	15.93	2.10
300	11.43	4.08	11.51	4.19
600	8.62	1.84	8.70	2.06

4 果穗振动仿真

4.1 不同采摘阶段的差异

分别对摘取和移送阶段果穗振动仿真模型进行激励加载运行,其中外伸穗轴长为 80 mm,夹持穗轴长为 35 mm,激励形式为 12 m/s^2 水平匀加速运动。对作用幅度为 100 mm 相应时刻的果粒摆角进行统计,摘取、移送阶段果粒摆角的正态分布如图 15 所示。

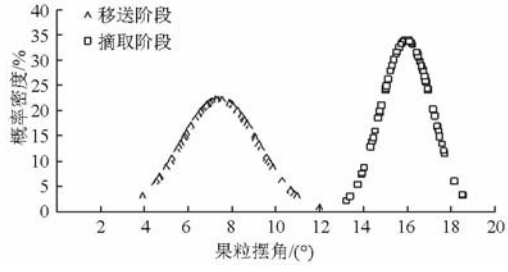

图 15 不同阶段果粒摆角统计

Fig. 15 Fruit swing angle at different stages

由图 15 发现,摘取阶段由于主穗轴与枝干的连接,末端的激励输入在果穗部位呈现杠杆放大效应,造成果粒的摆动程度显著大于移送阶段。

4.2 激励特性对果穗振动的影响

4.2.1 不同激励特性的仿真试验

对移送阶段果穗振动仿真模型,仍保持夹持果穗长为 35 mm,进行 3 类单因素仿真试验:

(1)分别进行加速度为 12 m/s^2 的水平与竖直加载运行,对 400 mm 激励幅度时刻的果粒摆角进行统计。

(2)分别进行 6、8、10、12 m/s^2 加速度水平下的水平加载运行,对 400 mm 激励幅度时刻的果粒摆角进行统计。

(3)在 12 m/s^2 水平加速度激励下,分别对 100、200、300、400 mm 不同激励幅度时刻的果粒摆角进

行统计。

4.2.2　果穗振动影响分析

（1）不同激励方向下的果粒摆角统计结果如图 16 所示，水平激励下果穗中所有果粒的累积摆角达到了 722.0°，与竖直激励下果穗中所有果粒的累积摆角 632.1°相比，水平激励对果穗振动的影响更大。

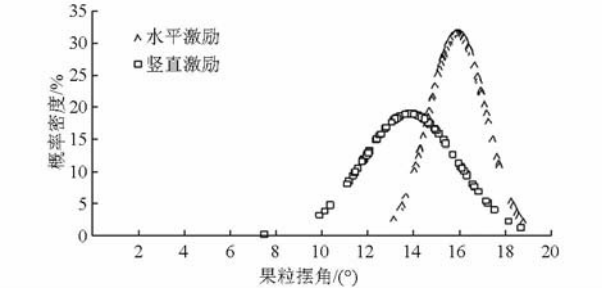

图 16　不同激励方向下的果粒摆角统计

Fig. 16　Fruit swing angle under different excitation directions

（2）在水平方向下，不同激励下的果粒摆角统计结果如图 17 所示，加速度为 6、8、10、12 m/s^2 下果穗中所有果粒的累积摆角分别为 236.5°、327.8°、559.0°、722.0°，激励越大，果穗的振动越严重。

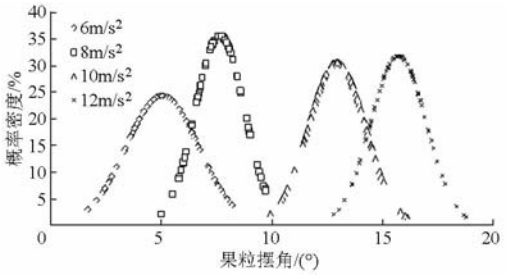

图 17　不同激励大小下的果粒摆角统计

Fig. 17　Fruit swing angle under different excitation values

（3）不同激励幅度下的果粒摆角统计结果如图 18 所示，激励幅度 100、200、300、400 mm 下果穗中所有果粒的累积摆角分别为 342.5°、468.9°、595.7°、722.0°，差异显著。由此可判断，在一定的方向与大小的激励输入下，激励幅度对于果穗的振动具有明显影响。

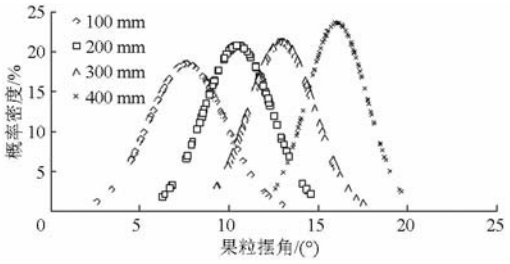

图 18　不同激励幅度下的果粒摆角统计

Fig. 18　Fruit swing angle under different excitation ranges

5　结论

（1）针对机器人穗轴夹剪采摘中的特殊激励特性，提出了“挠性杆-铰链-刚性杆-质量球”复合果穗模型，并通过试验获得了各模型元件的特性。

（2）通过梗系统 3D 扫描、挠性杆替换、果粒与梗间铰链的正态添加，建立了葡萄果穗振动仿真模型，不同阶段仿真运行的果穗各果粒摆角均值、标准差与验证试验结果相差均在 2% 和 6.6% 以内。

（3）果穗振动仿真分析表明，在同样激励作用下，摘取阶段果粒的摆动程度大于移送阶段；移送阶段的激励方向、激励大小以及幅度均对果穗振动具有显著影响。其中，水平激励较竖直激励产生的振动更为剧烈；激励大小、幅度均与振动程度成正比。

（4）该果穗振动仿真模型将大大推进果穗的机器人低脱落采摘研究，同时亦为机械振动收获等领域提供了仿真分析工具。仿真模型具有较高精度，但受现有方法所限，模型中尚未引入振动过程中果粒间的挤压碰撞因素。

参　考　文　献

1　刘继展，刘炜，毛罕平，等. 面向立柱栽培的移栽机器人设计与协调运动仿真[J]. 农业机械学报，2014，45(7)：48－53.
LIU Jizhan, LIU Wei, MAO Hanping, et al. Design and coordinated motion simulation of transplanting robot for column cultivation [J]. Transactions of the Chinese Society for Agricultural Machinery, 2014, 45(7): 48－53. (in Chinese)

2　SHIGEHIKO H, KENTA S, SATOSHI Y, et al. Evaluation of a strawberry-harvesting robot in a field test[J]. Biosystems Engineering, 2010, 105(2): 160－171.

3　张凯良，杨丽，张铁中. 草莓收获机器人采摘执行机构设计与试验[J]. 农业机械学报，2011，42(9)：155－161.
ZHANG Kailiang, YANG Li, ZHANG Tiezhong. Design and testing of picking and execution mechanism of strawberry harvesting robot[J]. Transactions of the Chinese Society for Agricultural Machinery, 2011, 42(9): 155－161. (in Chinese)

4　BULANON D M, KATAOKA T. A fruit detection system and an end effector for robotic harvesting of Fuji apples[J]. Agricultural Engineering International: CIGR Journal, 2010, 12(1): 203－210.

5　刘继展，徐秀琼，李萍萍. 果实采摘中果梗激光切割分析与实验[J]. 农业机械学报，2014，45(1)：59－64.
LIU Jizhan, XU Xiuqiong, LI Pingping. Analysis and experiment on laser cutting of fruit peduncles[J]. Transactions of the Chinese Society for Agricultural Machinery, 2014, 45(1): 59－64. (in Chinese)

6　刘继展，白欣欣，李萍萍，等. 果实快速夹持复合碰撞模型研究[J]. 农业机械学报，2014，45(4)：49－54.
LIU Jizhan, BAI Xinxin, LI Pingping, et al. Complex collision model in high-speed gripping of fruit [J]. Transactions of the Chinese Society for Agricultural Machinery, 2014, 45(4): 49－54. (in Chinese)

7 NAOSHI K, KOICHI T, TOMOWO S, et al. Path planning of tomato cluster harvesting robot for realizing low vibration and speedy transportation[J]. Engineering in Agriculture, Environment and Food,2009,2(3): 108 – 115.

8 UPADHYYAYA S K, RAND R H J, COOKE R. Dynamics of fruit tree trunk impact[J]. Transactions of the ASAE, 1981, 24(4): 846 – 855.

9 MOHAMED I G. Prediction of the suitable amplitude of shaking unit for fruit harvesting[J]. Misr Journal of Agriculture Engineering,2006,23(1): 1 – 18.

10 AWADY M N EL, GENAIDY MA L, RASHOWAN M. Modeling and simulating of olive-tree harvesting mechanism[J]. Misr Journal of Agriculture Engineering, 2008, 25(3): 712 – 722.

11 RAND R H, COOKE J R. Vibratory fruit harvesting: a linear theory of fruit-stem dynamics [J]. Journal of Agriculture Engineering Research,1970,15(4): 347 – 363.

12 BENTAHER H, HADDAR M, FAKHFAKH T. Finite elements modeling of olive tree mechanical harvesting using different shakers [J]. Trees, 2013, 27(6): 1537 – 1545.

13 COOKE J R, RAND R H. Vibratory fruit harvesting: a linear theory of fruit-stem dynamics [J]. Journal of Agriculture Engineering Research, 1969, 14(3):195 – 209.

14 PARCHOMCHUK P, COOKE J R. Vibratory harvesting: an experimental analysis of fruit – stem dynamics [J]. Transactions of the ASAE,1971,14(1): 20 – 24.

15 李永强, 杨学军, 王俊, 等. 基于 ADAMS 的酿酒葡萄植株受迫振动仿真研究[J]. 安徽农业科学, 2015, 43(27): 220 – 224.
LI Yongqiang, YANG Xuejun, WANG Jun, et al. Simulation of wine grape plants forced vibration based on ADAMS [J]. Journal of Anhui Agricultural Sciences, 2015, 43(27): 220 – 224. (in Chinese)

16 罗陆锋,邹湘军,熊俊涛,等. 自然环境下葡萄采摘机器人采摘点的自动定位 [J]. 农业工程学报,2015,31(2): 14 – 21.
LUO Lufeng, ZOU Xiangjun, XIONG Juntao, et al. Automatic positioning for picking point of grape picking robot in natural environment [J]. Transactions of the CSAE, 2015, 31(2): 14 – 21. (in Chinese)

17 卢俊.基于虚拟设计的采摘机构和视觉的关联定位[D].广州:华南农业大学,2009: 60 – 64.
LU Jun. The association positioning of picking-machine and vision based on virtual design[D]. Guangzhou: South China Agricultural University, 2009: 60 – 64. (in Chinese)

18 熊俊涛,邹湘军,陈丽娟,等.基于机器视觉的自然环境中成熟荔枝识别[J].农业机械学报,2011,42(9): 162 – 166.
XIONG Juntao, ZOU Xiangjun, CHEN Lijuan, et al. Recognition of mature litchi in natural environment based on machine vision [J]. Transactions of the Chinese Society for Agricultural Machinery, 2011, 42(9): 162 – 166. (in Chinese)

19 周祖锷. 农业物料学[M]. 北京: 农业出版社,1995.

20 王荣. 葡萄与番茄力学特性及机械损伤的研究[D]. 北京: 中国农业大学,2003.
WANG Rong. Research on the dynamical properties and mechanical damage of grape and tomato[D]. Beijing: China Agricultural University, 2003. (in Chinese)

21 王荣,焦群英,魏德强. 葡萄与番茄宏观力学特性参数的确定[J]. 农业工程学报, 2004, 20(2): 54 – 57.
WANG Rong, JIAO Qunying, WEI Deqiang. Determination of the macroscopic mechanical properties of grape and tomato [J]. Transactions of the CSAE, 2004, 20(2): 54 – 57. (in Chinese)

22 郭卫东. 虚拟样机技术与 ADAMS 应用实例教程[M]. 北京:北京航空航天大学出版社,2008.